ASTIA Doc. No. AD-152596
AFCRC-TR-58-246

ILLINOIS STATE WATER SURVEY
METEOROLOGIC LABORATORY
at the
UNIVERSITY OF ILLINOIS
Urbana, Illinois

EVALUATION OF THE AN/APQ-39(XA-3) CLOUD DETECTOR RADAR

by
K. E. Wilk

FINAL REPORT
on
Contract No. AF 19(604)-]395

March 16, 1955—March 31, 1958

The research reported in this document has been sponsored by the Geophysics Research Directorate of the Air Force Cambridge Research Center, Air Research and Development Command, Cambridge, Massachusetts.

ASTIA Doc. No. AD-152596
AFCRC-TR-58-246

Illinois State Water Survey
Meteorologic Laboratory
at the
University of Illinois
Urbana, Illinois

Evaluation of the AN/APQ-39(XA-3) Cloud Detector Radar

by

K. E. Wilk

FINAL REPORT

on

Contract No. AF 19(604)-1395

March 16, 1955 - March 31, 1958

G. E. Stout
Project Director

Wo Co Ackermann
Chief

The research reported in this document has been sponsored by the Geophysics Research Directorate of the Air Force Cambridge Research Center, Air Research and Development Command,, Cambridge, Massachusetts.

TABLE OF CONTENTS

LIST OF ILLUSTRATIOKS

LIST OF TABLES

ABSTRACT

This report is an evaluation of a ground based AN/APQ-39 (XA-3) airborne radar as a cloud indicator during the winter months in the Midwest. Data on clouds, precipitation, and other meteorological parameters were collected by means of a modified AN/APQ-39(XA-3) radar, meteorological instruments, and cloud photography. The observed data and radar characteristics are analyzed to determine the empirical detection capabilities, theoretical detection capabilities, and the synoptic interpretations of the radar echoes. The results indicate the AN/APQ-39 (XA-3) radar is capable of detecting 77 percent of the observed clouds. Cloud genera usually can be identified from the configuration of the radar return. The radar also provides limited knowledge of the existence and character of precipitation and of the air mass structure.

ACKNOWLEDGMENTS

This report was written under the direction of William C. Ackermann, Chief of the Illinois State Water Survey. Research was accomplished under the general guidance of the Project Director, Glenn E. Stout, Head, Meteorology Section.

The author wishes to express appreciation to Donald Staggs, Project Engineer, for the installation, maintenance and modification of the radar. Special credit is also due Jack E. Taylor, Meteorological Aide, for assistance in data collection and analysis.

Credit is due Ralph J. Donaldson, Jr., Geophysics Research Directorate, Air Force Cambridge Research Center and R. B. Leasure, Wright Air Development Center, for suggestions and guidance during the study.

INTRODUCTION

The problem of obtaining measurements of the vertical distribution of cloud and moisture through the troposphere confronts both the research and the operational meteorologist. Visual point observations are necessarily very subjective, and reinforce the need for better instrumentation. The ceiling light and ceilometer provide limited, but objective measurements of the lower limit of the cloud distribution. However, the determination of the vertical dimension relies mainly upon the analysis of occasional Rawinsonde data and observations from transitory aircraft.

The application of vertically pointing K-band radar as a cloud detector has been investigated in recent years. Excellent evaluations of 1.25 cm wavelength radar have been made by Plank, Atlas, and Paulsen, and Leasure and Thompson.[2]

This report follows the format of investigation of these studies but as applicable to 0.86 cm radar, which will hereafter be referred to as the APQ-39 radar.

History

The contract originated on March 16, 1955 as an in-flight

evaluation program of the APQ-39 airborne radar. After detailed planning, subsequent instrumentation and installation, final flight tests were attempted. In February 1956 the aircraft crashed with complete loss of equipment and personnel.

In September 1956, the initial program was revised by Supplemental Agreement No. 1 and in April 1957, by Supplemental Agreement Mo. 2. The latter revision directed the contractor to evaluate the APQ-39 radar as a ground-based unit.

The APQ-39 radar was transported from Wright Air Development Center to the University of Illinois Airport in Movember 1956. Installation of the equipment at the new location was completed in February 1957. The period from February 1957 to August 1957 was devoted to trouble shooting and the correction of numerous equipment malfunctions. Routine operation was attempted on several occasions, but equipment failures repeatedly interrupted data collection. The repetition of specific malfunctions indicated the need for a major change in equipment design. Personnel at Wright Air Development Center concurred and, in October 1957, an additional antenna was acquired. The modification to a twin antenna system and elimination of the duplexer was completed in December 1957. Routine data collection was carried on until February 28, 1958.

Evaluation Site

The evaluation of the APQ-39 radar was conducted at the Illinois State Water Survey Meteorologic Laboratory which is

located at the University of Illinois Airport (CMI). The site is five miles south of Champaign, 75 miles east-northeast of Springfield, and 83 miles southeast of Peoria. The surrounding area is primarily rural with no significant variations in terrain elevation.

The Gulf of Mexico provides the principal source of moisture advected over Illinois. The average monthly occurrence of cyclone centers in the state, as shown in Figure 1, reaches a maximum in January with a secondary peak in March. The average cloudiness as reported by ground observers,[3] shows the relative monthly distribution of the major cloud types, Figure 2.

Radar Installation

The radar was installed in a "window" mounting between the TPS-10 and CPS-9 towers, as shown in Figure 3. The enclosed antenna housing in the enlarged portion of Figure 3 constituted the original installation before modification to a twin antenna system. After removal of the duplexer, it became the receiver unit. The open antenna on the left surmounts the remoted transmitter unit.

The interior installation of the radar components is shown in Figure 4. The cables running to the opening in the upper left of Figure 4c lead to the receiver, Figure 4a, and the transmitter, Figure 4b.

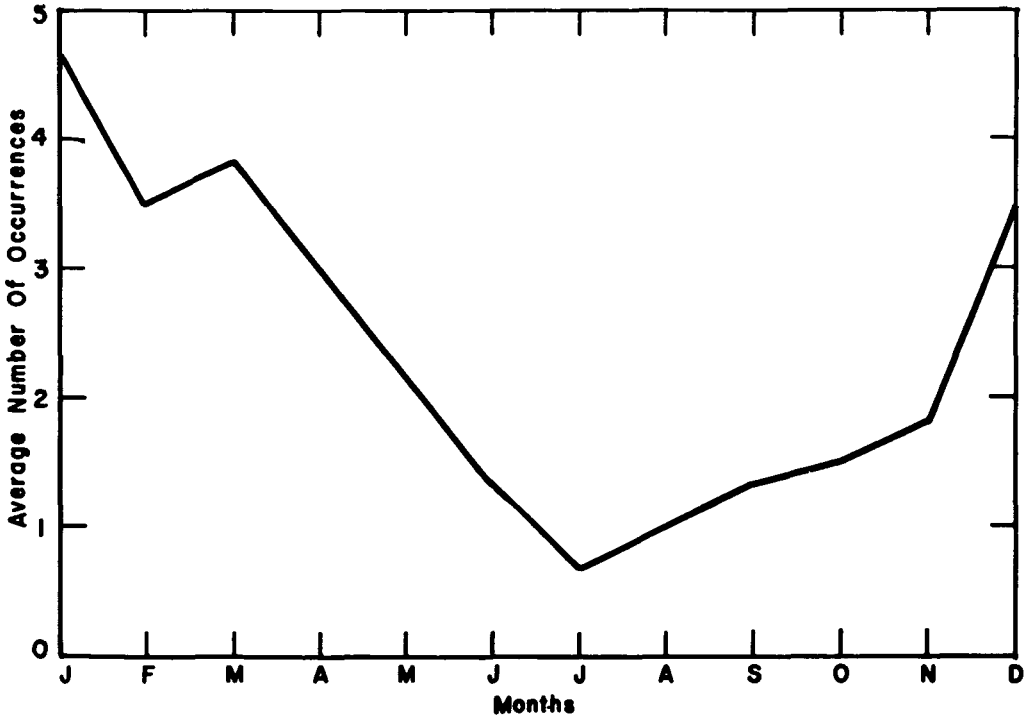

FIG. 1 AVERAGE MONTHLY OCCURRENCE OF CYCLONE CENTERS ILLINOIS, 1949-1955

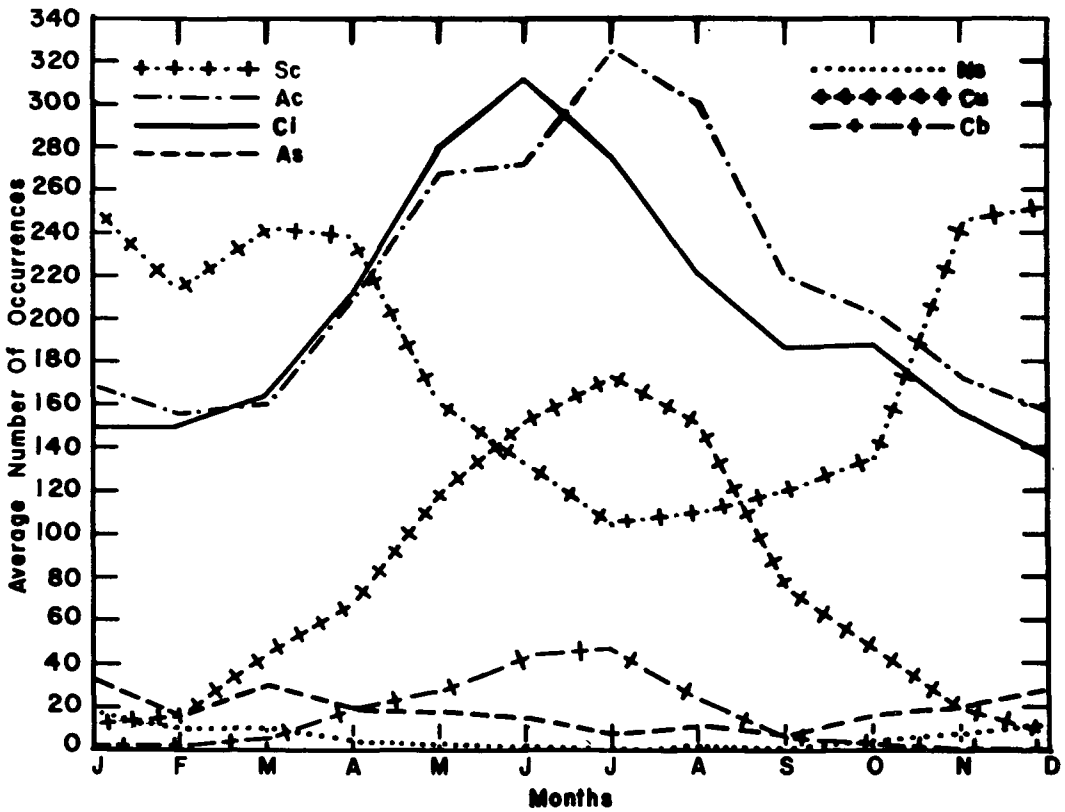

FIG. 2 AVERAGE MONTHLY HOURLY CLOUD OCCURRENCES SPRINGFIELD, ILLINOIS 1949-1955

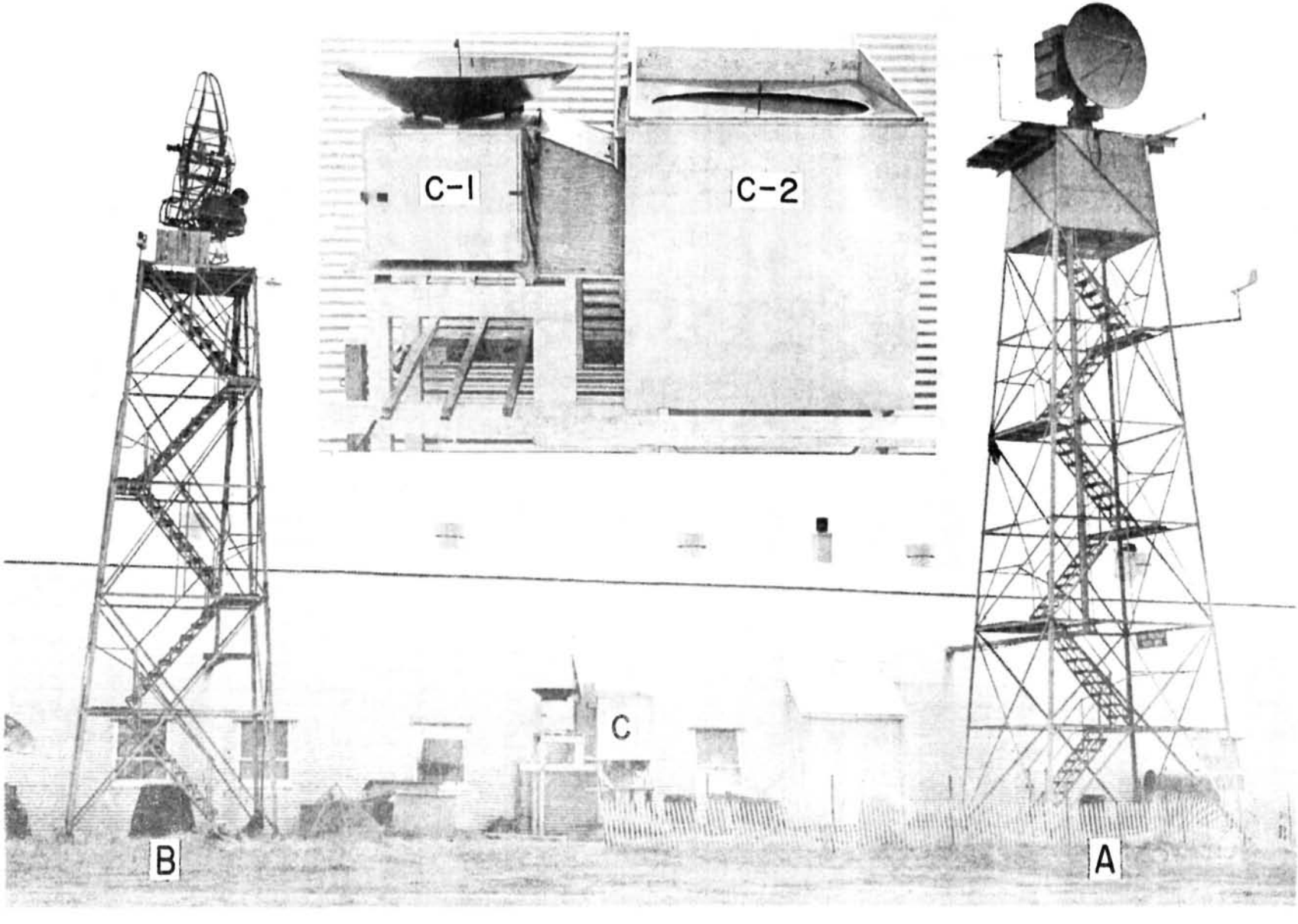

FIG. 3 AN/APQ-39 RADAR INSTALLATION

A. CPS-9 Radar Tower, B. TPS-10 Radar Tower, C. AN/APQ Radar Set — Insert, C-1. Transmitter, C-2. Receiver

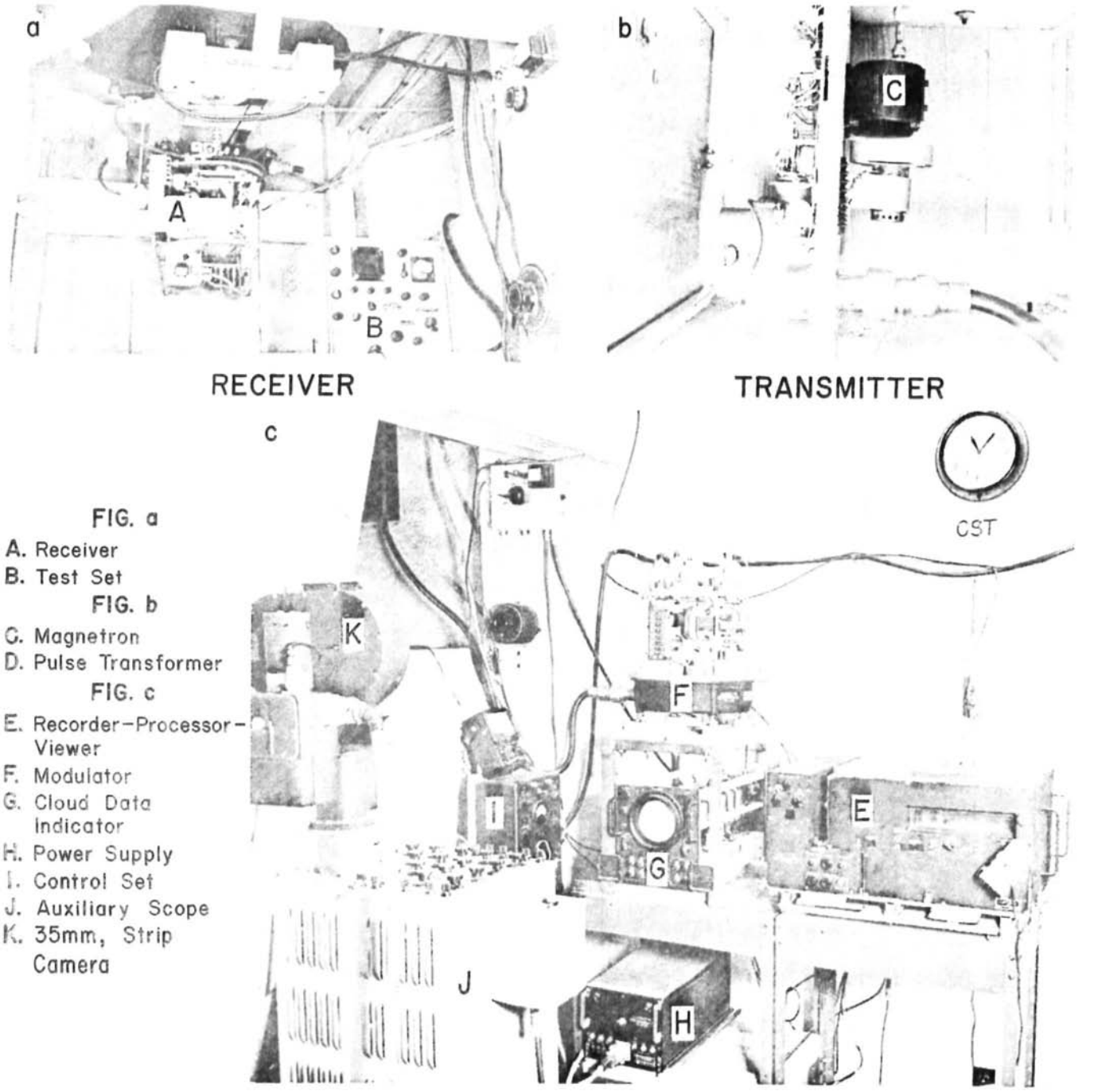

FIG. 4 AN/APQ-39 RADAR (MODIFIED)

Radar Characteristics

The principal characteristics of the APQ-39 radar are as follows:

		Value
1.	Frequency (mean)	34.5 Kmc
2.	Power Output	
	Peak	9.18 kw*
	Average	5.01 watts
3.	Pulse Width	0.8 μ sec.
4.	Pulse Repetition Rate	683 pps
5.	Receiver Bandwidth	1.5 mcs
6.	Receiver I-F Frequency	30 mcs
7.	Receiver Sensitivity	-100 dbm
8.	Beam Width	0.6 degrees
9.	Wavelength	0.86 cm

Beam Collimation

Repeated failures of the crystal, TR tube, and ATR tube suggested the elimination of the duplexer and resulted in the decision to use a twin antenna installation.

The use of separate antennas for transmitting and receiving required approximate beam coincidence. Theoretical considerations based on results obtained by Robbiani and Swingle, emphasized the need for variable antenna tilt so as to hold the signal loss to a prescribed minimum. For example, conceding a received signal loss of one db, it would be necessary to employ three antenna tilt angles in order to cover a height interval of 840 to 60,000 feet. However, predetermination of the desired height subdivisions was very difficult since the vertical distribution of the targets was unknown. Also, in many

*The peak power output was measured with the AN/UPM-14(XN-14) Test Set and directional couplero Values as high as 16 kw have been measured by Aerial Reconnaissance Laboratory, Wright Air Development Center.

instances it was necessary to sample widely spaced intervals in the vertical depending on the synoptic conditionso Therefore, in the APQ-39 evaluation, a compromise was established between height intervals and received signal loss. Two antenna tilt angles were selected. On "high" tilt a one db loss existed between 3200 and 30,000 feet. On "low" tilt a one db and two db loss occurred at the upper (3200 feet) and lower (1200 feet) extremes, respectively. The acceptance of a two db loss at 1200 feet seemed justified considering that this low level afforded less range and intervening target attenuation. Also, the precipitation type target common to the extreme lower levels has a high threshold of detectability. Antenna tilt was checked empirically using optimum detection of cloud and precipitation targets at the two predetermined levels (approximately 2300 and 6700 feet) corresponding to zero received signal loss.

THEORETICAL DETECTION CAPABILITIES

Before considering the empirical data analysis, it is useful to gain an a priori understanding of the theoretical aspects of the APQ-39 radar capabilities. Although numerous assumptions must be made in the following evaluation, the role of individual radar characteristics and the importance of moisture variation becomes more evident.

Also, since many of the values of the radar and

atmospheric parameters used exceed the practical accuracy obtainable, it is obvious that the numerical conclusions cannot be taken as absolute, but only as relative.

Minimum Detectable Reflectivity

The basic radar - range equation of Austin[5] is used in the following to define the minimum detectable reflectivity of the 0.86 cm radar.

$$\bar{P}_r = \left[6.1 \times 10^{-16} P_t G^2 \lambda^2 \phi\theta h\right] \frac{\eta\kappa}{R^2} = C \frac{\eta\kappa}{R^2}$$

where: $\bar{P}_r$, average echo power, watts

P_t, peak transmitted power = 9.18×10^3 watts

G, antenna gain = 9.2×10

λ, wave length = 0.86 cm

ϕ, θ, effective beam widths = 0.60 degrees

h, pulse length = 240 meters

η, reflectivity per unit volume, cm^{-1}

κ, transmission factor

R, target range, km

evaluating C:

$$C = 6.1 \times 10^{-16} p_t G^2 \lambda^2 \phi\theta h = 3.03$$

solving for η :

$$\eta = \frac{\bar{P}_r R^2}{C\kappa}$$

converting E to μ seconds and $\bar{P}_r$ to milliwatts:

$$\eta = \frac{\bar{P}_r R^2}{C_1 \kappa}, \quad \text{where } C_1 = C(\mu\text{sec/km})^2(10^3)$$

$$\text{where } C_1 = 134.5 \times 10^3$$

taking logarithms:

$$10 \log \eta = -10 \log C_1 + 20 \log R \mu \sec + S + A$$

where S, measured receiver sensitivity = -100 dbm

A, attenuation

inserting values for C, and S:

$$10 \log \eta = -151.28 + 20 \log R + A$$

which expresses the minimum detectable reflectivity as a function of range.

Determination of A: at any one range,

$$A = A_{wv} + A_{cld} + A_p$$

where: A_{wv} is attenuation by atmospheric water vapor (W_{wv}),

A_{cld} is attenuation by intervening cloud (W_{cld}),

A_p is attenuation by precipitation (W_p).

Values of W_{wv} applicable to various types of Midwest air masses are approximated as follows:

Air mass	Water vapor content average to 400 mb
Pc, winter, polar Canadian	0.5 g/m^3
Pc, summer, polar Canadian	3.6 g/m^3
Npp, winter, modified maritime polar	1.7 g/m^3
Tg, winter, Gulf	7.5 g/m^3
Tg, summer, Gulf	12.7 g/m^3

Values of cloud liquid water content are obtained from Diem's cloud drop samples.

Cloud type	Average water content
Cumulus	0.50 g/m3
Stratocumulus	0.13 g/m^3
Stratus	0.19 g/m^3
Altostratus - Altocumulus	0.22 g/m^3
Nimbo stratus	0.31 g/m^3

Figures 5 and 6, which are based upon work by Ryde,[7] express W_{wv} and W_{cld} in terms of attenuation at 0.86 cm wavelength.

Haddock[8] has determined A_p as a function of W_p where W_p is expressed in surface rainfall rate. The relationship has an approximate value of 0.07 db/1000 feet/mm/hour and is assumed applicable to the freezing level.

Thus, minimum detectable reflectivity values can be calculated assuming various ranges and various synoptic conditions, and compared to the reflectivity from various cloud types.

Cloud Reflectivity

Rayleigh scattering and Diem's cloud drop data are used to determine cloud reflectivity.

For Rayleigh scattering,

$$\eta_1 = \frac{\pi^5}{\lambda^4}\left[\frac{m^2-1}{m^2+2}\right]^2 Z$$

where: η_1 = reflectivity, (cm^{-1})

m = refractive index

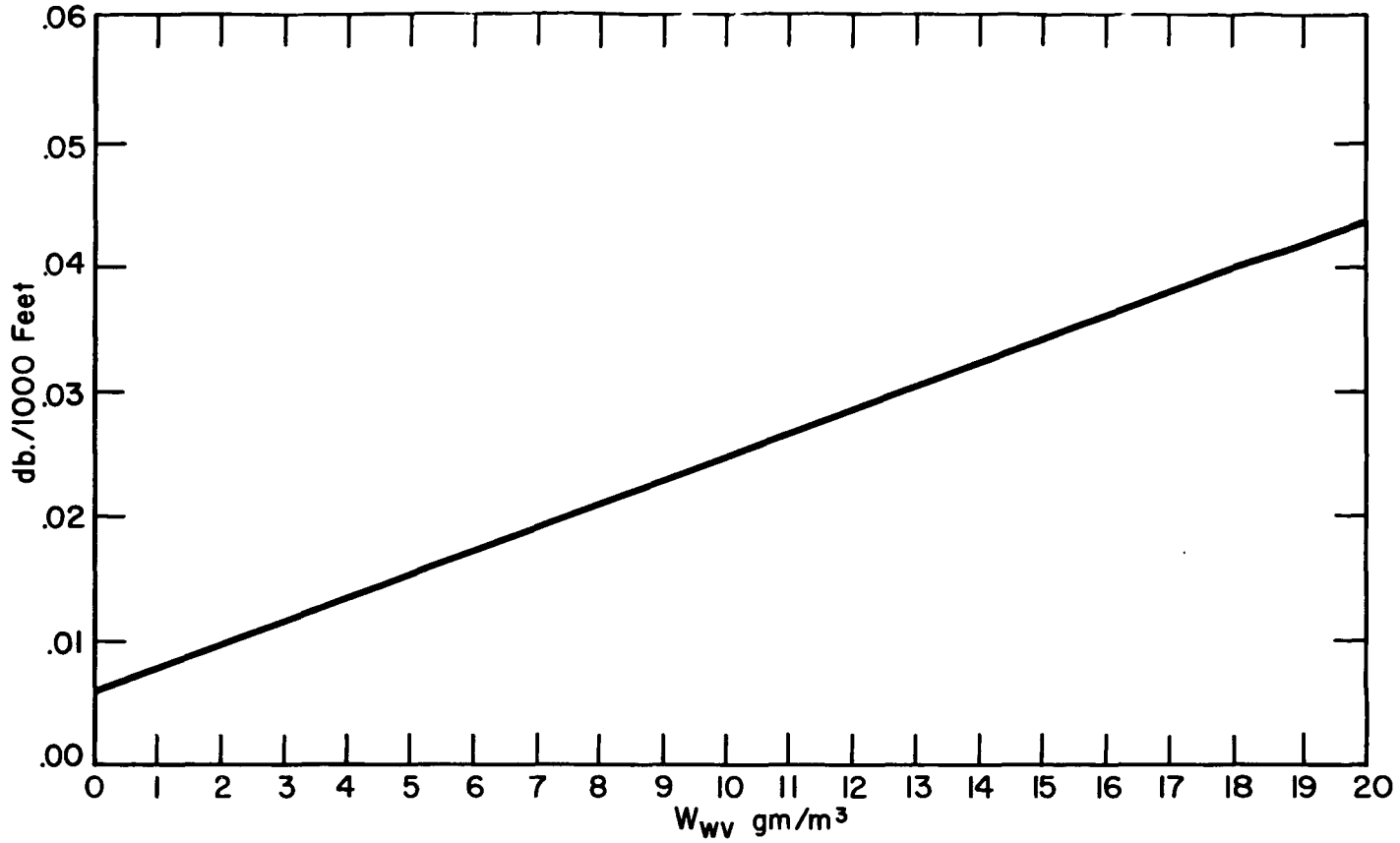

FIG. 5 ATTENUATION BY WATER VAPOR AND OXYGEN (AFTER RYDE)
ONE WAY ATTENUATION AT λ = 0.86cm.

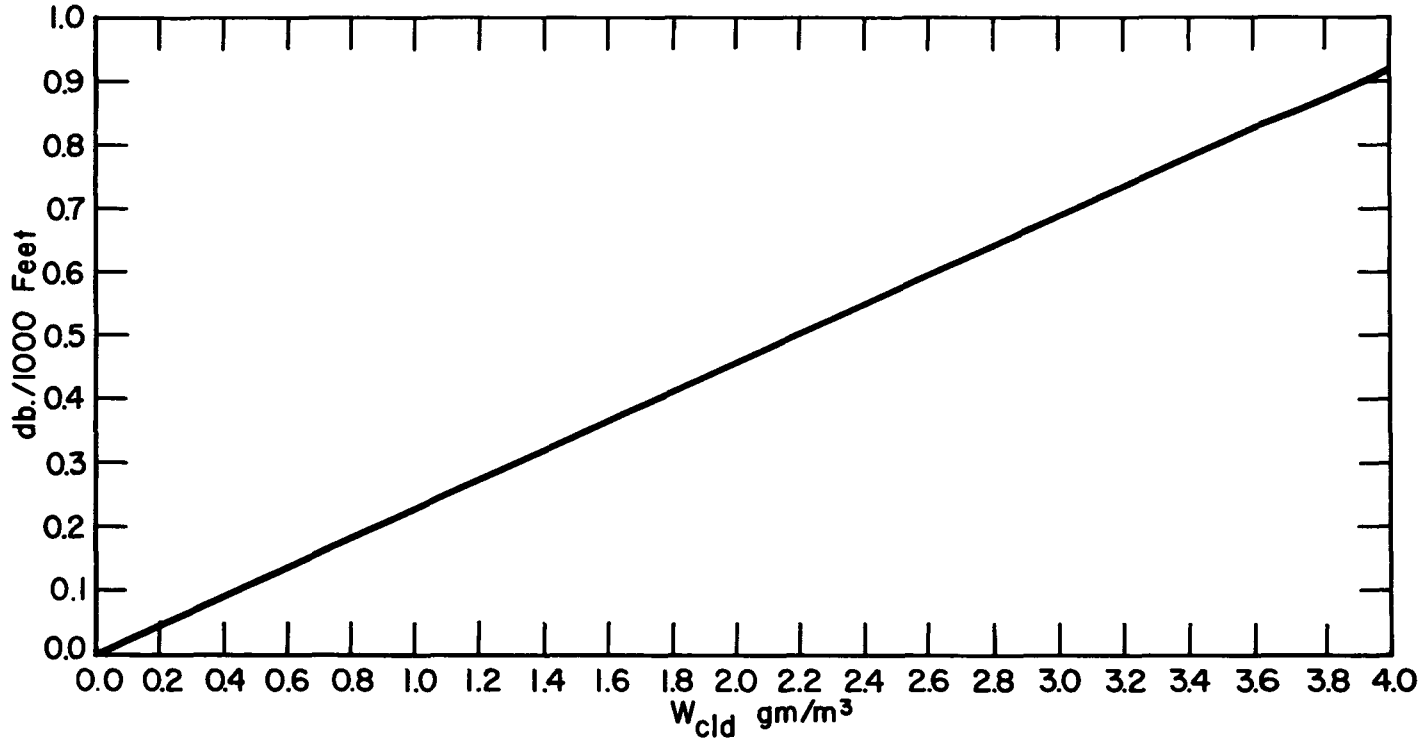

FIG. 6 ATTENUATION IN CLOUD (AFTER RYDE)
ONE WAY ATTENUATION AT λ = 0.86cm.

λ = wavelength, (cm)

Z = function of the number and diameter of the particles, (μ 6/m3).

The quantity $(m^2-1)^2/(m^2+2)^2$ has a value of 0.89 at λ = 0.86 cm.

evaluating: $\eta 1 = 4.94 \times 10^{-28} Z$ (for water)

Bartnoff and Atlas [9] have found that,

$$Z = \frac{6G}{\pi e} d_o^3 W(10^{12})$$

where: G, a dimensionless factor, has a preferred value of 1.35

e, density of particles (g/cm^3) has a value of 1 for water

d_o, median volume diameter (μ)

W, liquid water content, (g/m^3)

10 , constant for converting Z to units of μ^6/m^3

then:

$$\eta_1 = 12.85 \times 10^{-16} d_o^3 W$$

and:

$$10 \log \eta 1 = -148.9 + 30 \log d_o + 10 \log W$$

which expresses cloud reflectivity as a function of median volume diameter and liquid water content.

Using Diem's cloud drop samples, the cloud reflectivities were computed. Table 1 lists values of 10 log $\eta 1$ for various cloud types.

TABLE I

CLOUD REFLECTIVITY FOR 0.86 cm RADAR

Cloud Type	$30 \log \bar{d}_o$	$10 \log \bar{w}$	$10 \log \eta 1$
	microns	g/m^3	db
1. Stratus	34.5	-7.2	-121.6
2. Altostratus-Altocumulus	34.5	-6.6	-121.0
3. Stratocumulus	31.4	-8.9	-126.4
4. $Cumulus_1$	35.4	-4.4	-117.9
5. $Cumulus_2$	35.9	-3.0	-116.0
6. Nimbostratus	39.0	-5.1	-115.0

Individual cloud detectability can be expressed as a function of maximum detectable range assuming various air masses and vertical moisture distributions. Table 2 illustrates the importance of the parameters in the determination of maximum detectable range.

For example, assume a synoptic situation consisting of a semi-tropical air mass in summer with a single As-ac cloud layer from 14,000 to 16,000 feet. As can be seen from Table I, the cloud reflectivity would be -121.0 db. The minimum radar detectable signal at a range of 15,000 feet (approximately 28.4 micro-seconds) would require a reflectivity of -122.2 db neglecting attenuation. Considering the attenuation by the water vapor (Figure 5) of the air mass whose average liquid

TABLE 2

DETERMINATION-OF MAXIMUM DETECTABLE RANGE

Air Mass	1. Pc, polar Canadian, winter and summer 2. Npp, modified mP, central U. S., winter 3. Tg, mT, Gulf, winter and summer
W_{wv}	1. Pc, winter, 0.5 g/m^3 Pc, summer, 3.6 g/m^3 2. Npp, winter, 1.7 g/m^3 (Average from SFC to 400 mb) 3. Tg, winter, 7.5 g/m^3, Tg, summer, 12.7 g/m^3
W_{cld}	Diem's cloud samples, g/m^3 Cu 0.36; Cu 0.50; Sc 0.13; St 0.19; As-Ac 0.22; Ns 0.31
W_P	Rain, mm/hr
A_{wv}	Figure 5 (one way attenuation)
A_{cld}	Figure 6 (one way attenuation)
A_P	Rain, 0.07 db/1000 ft/mm/hr to $h_{t \geq OCC}$ (one way attenuation)
A	$A_{wv} + A_{cld} + A_p$
Maximum Detectable Range	$10 \log \eta_1 = -151.28 + 20 \log \mu sec + A$

water content is 12.7 g per cubic meter, the required reflectivity would then become -121.1 db and therefore the cloud would be detectable. However, if a layer of stratocumulus were present from 1500 to 5500 feet, an additional factor of attenuation due to the intervening cloud would increase the required reflectivity by 0.2 db which would result in the upper layer becoming nondetectable.

Although the individual attenuation effects caused by water vapor, intervening cloud, and precipitation are extremely small, the cumulative effect on a target which is already near the threshold of detectability can be critical. Obviously, the range factor is by far the most important parameter to consider. However, one must also consider the intervening environment of the target in evaluating the capabilities and limitations of the cloud detection radar.

EMPIRICAL DETECTION CAPABILITIES

Control Data

The evaluation of the APQ-39 radar was accomplished by integrating the various control data into target definition. Analysis of the radar echo required the knowledge of several basic parameters concerning the target and its environment. Table 3 lists the control data, the source, and the order of acceptance of the source,,

TABLE 3

CONTROL DATA COLLECTION

	SOURCE			
PARAMETERS	Pibal	Skew-T Diagram	Dome Camera	Pilot Report	Service "A" and Local Observations
Freezing Level		1		2	
Temperature Inversion		1		2	
Air Mass Identity		1			
Cloud Temperature		2		1	
Cloud Top		2		1	
Cloud Base	2	4		1	3
Cloud Amount		4	2	3	1
Cloud Type		3	2		1

Cloud types and amounts were extracted at 30-minute intervals from the dome camera film or from local observations. Cloud heights were obtained from local observations. Pilot reports and balloon observations vere used when considered representative of the conditions in the local area. The two daily Radiosonde observations from the Weather Bureau station

at Peoria were independently analyzed and the data applied for a period of one to six hours, depending on the stability of the synoptic conditions. The skew-T, log P diagram cloud analysis was held as objective as possible, using the pre-selected criteria listed in Table 4.

TABLE 4

SKSW-T, LOG P DIAGRAM CLOUD ANALYSIS

Cloud Type	Cloud Base	Cloud Top	Cloud Amount
Low and Middle Stratified	3°C temp, dew pt. spread	3°C temp, dew pt. spread	Temp, dew pt. spread
Low Convective	Convective - Condensation-Level	Level of decrease in positive area	0^{o}C to 3^{o}C overcast 3°C to 5°C broken
Middle Convective	Level of Free Convection	Top of positive area or 3°C temp, dew pt. spread	5°C to 7°C scattered
High Stratified and Convective	Average of height of -40°C isotherm and 90% humidity-contrail curve	Height of tropopause minus 2000 feet	

Radar Data Collection

Since the APQ-39 was designed as an airborne radar, airborne application of results obtained in a ground-based evaluation is limited. However, to simulate airborne presentation, data were collected simultaneously with two continuous strip cameras. One camera employed a film speed of approximately one inch per fifteen

minutes with a fixed vertical scale of 50,000 feet. The second camera operated at a film speed of approximately one and one-half inches per minute with a variable vertical scale. The presentation on the slow moving film approximates that of the fast camera in an aircraft flying 22.5 times the target velocity. Also, for analysis purposes, the dual data collection permitted examination of the echo both in detail and composite form.

Radar Data Analysis

The radar presentation was analyzed at 30-minute intervals. Individual echoes, or layers of echo, were examined for measurements of bases, tops, horizontal continuity, and vertical character. Additional information, such as slope, uniformity of bases and tops, and sharpness of boundary, was extracted as an average, applicable to the total period of operation.

A total of 34 days of APQ-39 radar data was analyzed in this manner. The choice of 30-^inute intervals for data extraction was for two reasons. First, numerous equipment malfunctions resulted in sporadic data collection until the second antenna installation in December 1957. Consequently, the treatment of days as separate cases with singular observations was not possible. Secondly, the wide variations of the targets in time and space seemed to justify, if not necessitate, the use of a short time interval. Therefore, each 33-minute radar observation was assumed to be independent and evaluated as a single case.

Cloud Detectability

Table 5 summarizes the 561 cases investigated for the nine types of targets observed. It was found that 77 percent of all observed clouds were detectable. Since most of the cases represent wintertime conditions, the results may not be applicable to the other three seasons. The detectability of cumulus, for example, was definitely biased by the large percentage occurrence of associated precipitation.

The number of detectable cases in maritime and continental air reflects the comparative number of occurrences of the cloud in the air masses. As would be expected, the majority of the observed total cloudiness is associated with the maritime condition. However, the magnitude of the contrast is somewhat unreal. The high wintertime occurrence of low cloud in continental air resulted in the surface observer's inability to see and identify any middle or high cloud which might have been present.

The slight difference in the percentage detectability in the two types of air masses is not significant. Although one might suspect that maritime air would require a higher minimum detectable signal because of the increase.in attenuation due to water vapor.

The effect of target temperature appears to be indicative of the variance expected between winter and summer conditions. Both stratocumulus and altocumulus-altostratus exhibit better detectability at lower temperatures. However, temperature

TABLE 5

CLOUD DETECTAMLm

CLOUD TIPE	Number of Detectable Cases	Number of Non-detectable Cases	Total Percentage Detectable	Number of Detectable Cases in Maritime Air	Number of Detectable Cases in Continental Air	Percentage Detectability in Maritime Air	Percentage Detectability in Continental Air	Mean Range of Detectable Cases	Mean Range of Non-detectable Cases	Mean Temperature of Detectable Cases - °C	Mean Temperature of Non-detectable Cases - °C	Mean Thickness of Detectable Cases	Mean Thickness of Non-detectable Cases	Mean Estimated Cloud Base	Mean Estimated Cloud Top	Mean Radar Echo Base	Mean Radar Echo Top	Number of Cases with Surface Precipitation	Percentage of Cases with Surface Precipitation
LOW																			
"Stratus	106	0	100	21	85	100	100	9*		+0	-	33*		9*	42*	27*	53*	28	26
Stratocumulus	102	25	80	66	36	85	73	27	29*	-6	+1	26	25*	27	53	34	61	12	9
Cumulue	10	9	53	7	3	50	60	22	17	+5	-	23	13	22	45	-	51	6	60
Niabostratus	17	0	100	12	5	100	100	21	-	-5	-	97		21	118	-	99	6	35
TOTAL	235	34	87	106	129	85	90	20	28	-2	45		19	20	65	-	66	52	19
MIDLLK										1									
Altocumulus	30	28	52	19	11	43	79	120	90	-18	-	'38	-	120	158	125	149	5	9
Altostratua	38	5	88	30	8	85	100	108		-		-	-	108	-	130	189	4	9
Altocumulus-Altostratua	71	13	85	64	7	88	64	98	74	-11	-1	12	4	98	110	115	151	17	20
TOTAL	139	46	75	113	26	74	79	109	82	-15		25	4	109	134	123	162	26	14
HIGH																			
Cirrus	22	35	39	27	5	55	63	304	289	-45	-44	22	51	304	326	213	253		
Cirrostratus	36	14	72	30	6	68	100	218	230	-41	-40	93	94	218	311	221	251		
TOTAL	58	49	54	57	11	38	33	261	260	-43	-42	56	73	261	319	217	252		
TOTAL ALL CLOUDS	432	129	77	276	166	75	87												

*feet x 10^2

observations of the other cloud types were too limited to support of deny this relationship or to suggest a liminal value.

There is little apparent relationship between target thickness and detectability. This is understandable when one considers the pulse length of the APQ-39 radar. Assuming a filled beam volume, the minimum thickness of a threshold target would be approximately 480 feet. Cloud layers and measurements which approached this condition were too infrequent to illustrate the effect of thickness. On the other hand, one would suspect that the drop size would be directly related to the cloud thickness. This factor is apparent in the case of cumulus in which the mean thickness of the detectable cases is 1000 feet greater than that of the non-detectable cases.

The comparison between estimated cloud bases and tops and radar echo bases and tops does not directly represent deviation between target and indicated target dimensions. The cloud parameters were observed or in some cases, forecasted, using the criteria listed previously. Therefore the evaluation is related mainly to the observational technique involved.

The limited number of balloon and aircraft measurements with associated radar data are listed separately in Table 6. On many occasions the two observations were widely separated in space depending on the drift of the balloon and the height of the target. Since radar echo base fluctuations of 500 feet per minute were not uncommon, the probable deviation of

measurement is within 500 feet. Therefore, it appears that the integrated echo base is a more representative measurement than the point balloon observation.

TABLE 6

MEASUREMENT OF CLOUD BASES AND TOPS

CLOUD BASE MEASUREMENTS		CLOUD TOP MEASUREMENTS	
BALLOON	RADAR	AIRCRAFT	RADAR
ft. x 10^2	ft. x 10^2	ft. x 10^2	ft. x 10^2
147	150	240	270
144	130	220	230
114	130	90	80
81	90	70	40
48	45	63	50
38	35	45	26
27	30	34	35
26	35	20	15
20	15		

The echo-cloud top relationship shows more deviation. However, there was great time and space separation in the data. Also, the small number of observations for comparison prevents the assigning of absolute values to the base and top deviations. Further evaluation should be made on an operational basis where numerous detailed aircraft reports are available.

Detection of Precipitation

The APQ-39 radar is extremely sensitive to the detection of surface precipitation. Signal return is visible when rainfall rates are below the resolution of a standard recording raingage. Rainfall rates of one mm/hr and greater produce a saturated signal. The return from snow is somewhat weaker with the minimum detectable rate quite variable.

The effect of rain attenuation becomes noticeable when the rate exceeds five mm/hr. In one case, the detectable top lowered from 20,000 feet to 15,000 feet. Naturally, this example cannot be extrapolated since the target detectability above the precipitation is important. Although high rainfall rates were not experienced, it can be assumed that the effect would be very detrimental to upper cloud detection. In this respect, in-flight radar operation would be more favorable for cloud detection than would a ground-based installation. The precipitation normally would constitute the terminal target and therefore reduce the consequences of the attenuation. In either case, the important problem is to distinguish between cloud base and precipitation. The differentiation is usually impossible. However, it is feasible in certain cases where cloud is detected before the start of precipitation. By reducing the receiver gain until the target is just visible, the encounter of rain becomes evident due to the saturated condition of its signal.

Also, precipitation during the wintertime generally will display greater uniformity in stratified conditions. The separation in low level shower activity is normally impossible. The only indicator is the echo's proximity to the surface.

Cloud Differentiation

Examples of seven of the basic cloud genera and their respective radar presentations are illustrated in Figures 7 through 9.

Figure 7a show's a layer of stratocumulus with its typical undulating and rounded elements as portrayed by the dome camera. The associated radar echo reflects its gentle, rolling action with a stratified texture arranged in constrained vertical developments. Stratocumulus can be differentiated from the wintertime cumulus example in Figure 7b by the minute cellular texture of the cumulus. Echo from wintertime cumulus often exhibits a "no return" or weak layer, as shown in this example between 5000 and 7500 feet. The cloud base and light precipitation are evident to 5000 feet with the top strongly outlined from 7500 to approximately 9000 feet. The echo from stratus in Figure 7c is easily identified by the height, uniformity, and the continuous nature of the base and top.

Figure 8 illustrates the characteristic patterns of middle clouds. In Figures 8a and 8b note the similarity of the altocumulus and altostratus echo to the stratocumulus and stratus echo in Figures 7a and 7c, respectively. The combined middle

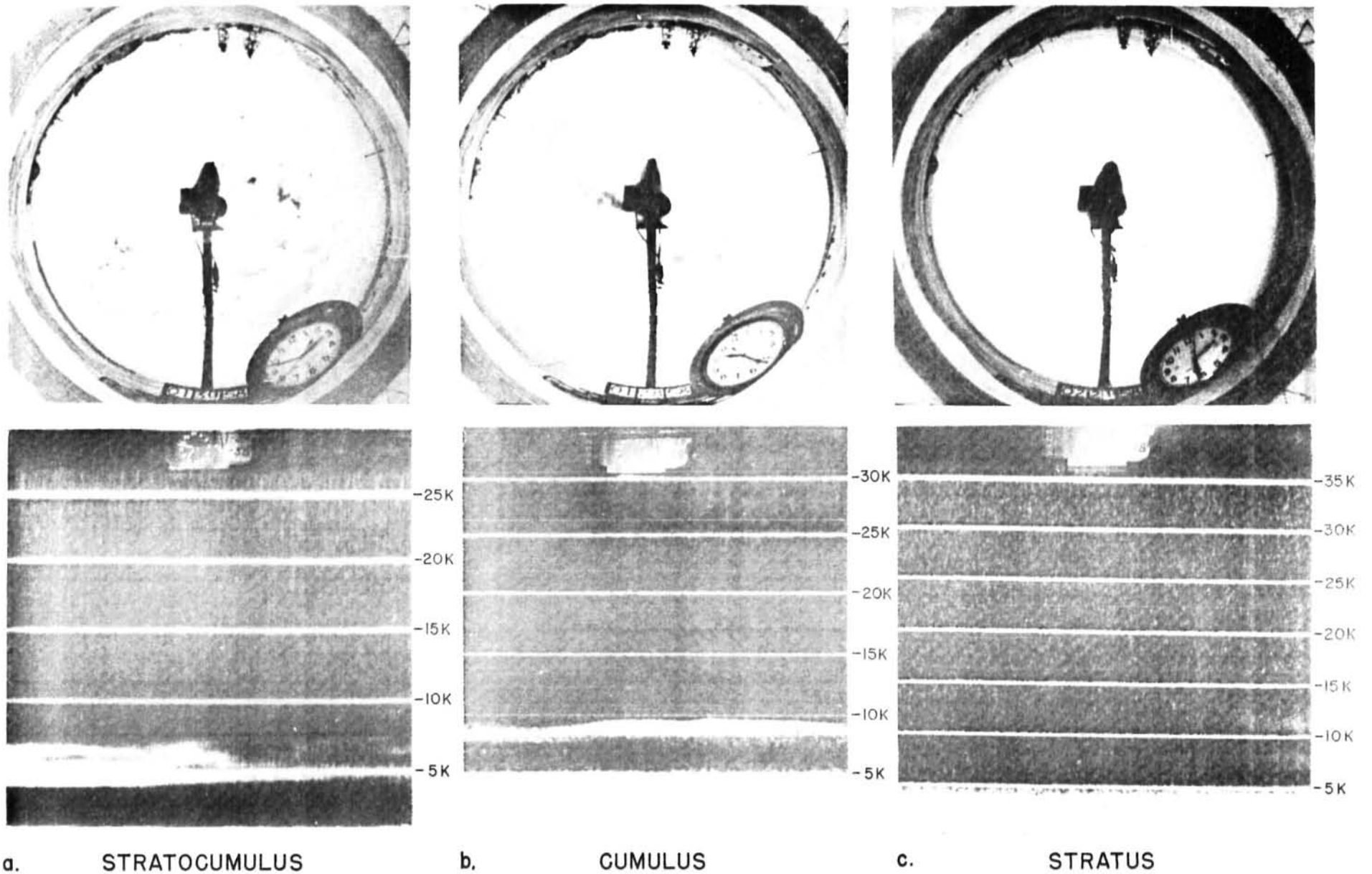

FIG. 7 LOW CLOUD AND ASSOCIATED RADAR ECHO

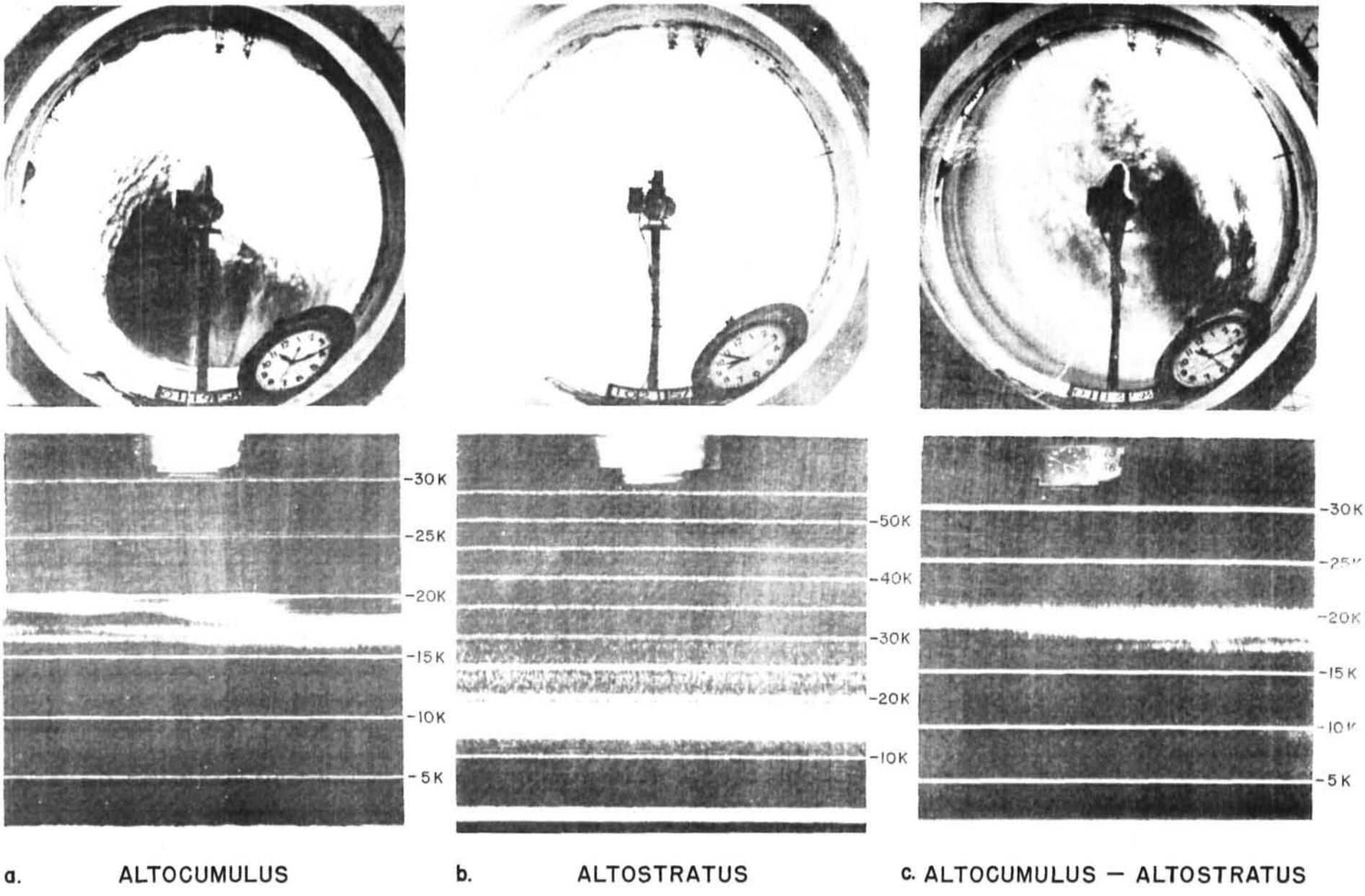

FIG. 8 MIDDLE CLOUD AND ASSOCIATED RADAR ECHO

cloud example in Figure 8c incorporates the uniformity of the altostratus with the texture of the altocumulus.

The high cloud examples in Figure 9 are more difficult to differentiate. The cirrostratus uniformity in Figure 9a is slightly more evident when compared to the more cellular nature of the cirrocumulus in Figure 9b.

It appears that normal cloud observation criteria, e.g. height, structure, and texture, are applicable to echo interpretation. Trained observers should experience little difficulty in identifying cloud genera.

However, no attempt should be made to determine cloud species or varieties. These classifications are based on luminance, transparency, and the arrangement of microscopic elements, and are not apparently analogous to any echo characteristics.

Invisible Targets

Occasionally, the APQ-39 detects targets apparently invisible to a ground observer. These echoes, normally referred to as "angels", occur at the lower levels and seldom exceed 7000 feet. They have been found to be more prevalent in early afternoon, but have been detected at all hours. There is no apparent association with the prevailing cloud. "Angels" have been detected on days with low cloud as well as on clear days. Figure 9c illustrates a clear sky example of angel occurrence. No theoretical or empirical explanation as to the nature

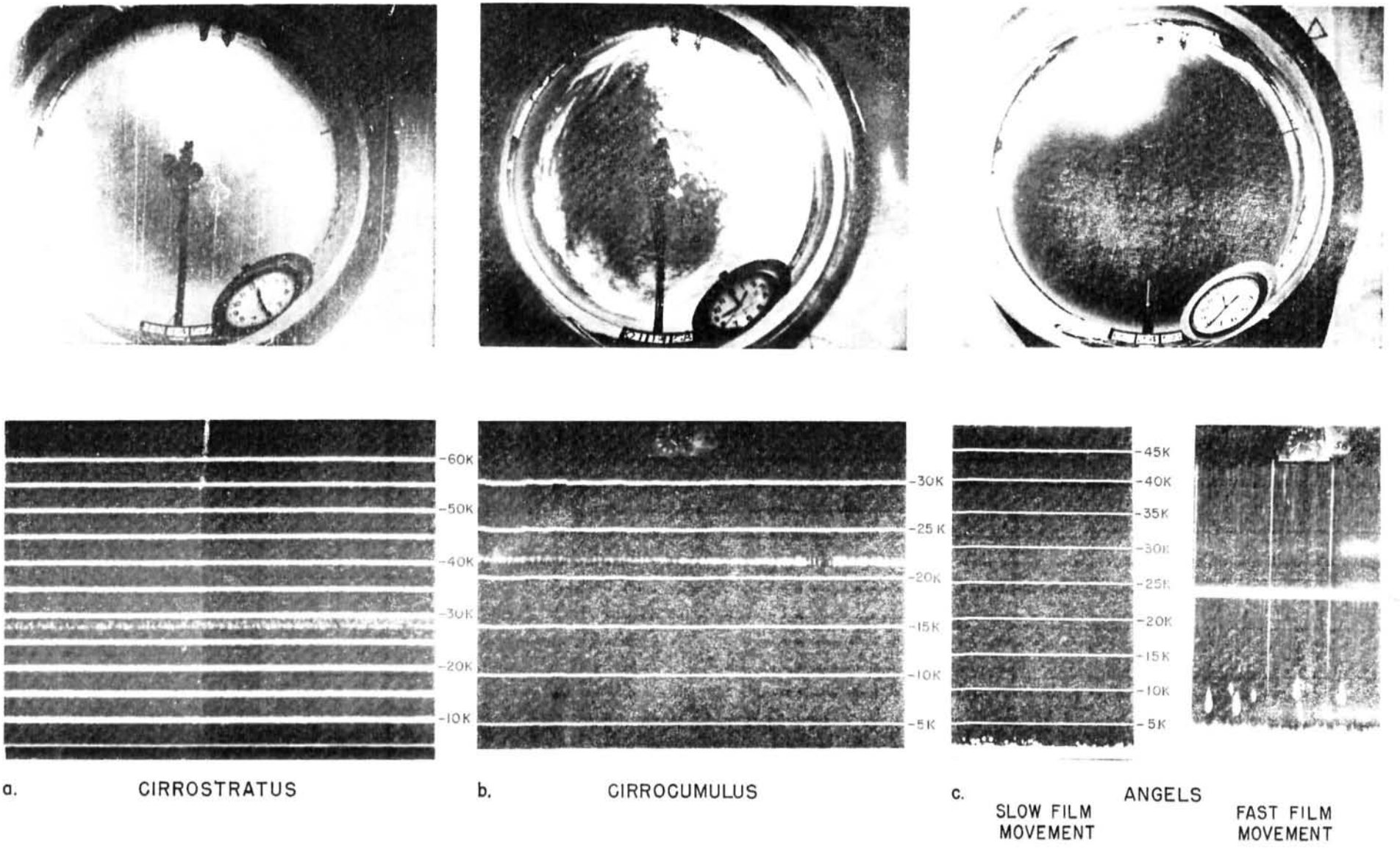

FIG. 9 HIGH CLOUD AND ANGELS AND ASSOCIATED RADAR ECHOES

or cause of this phenomena is offered in this evaluation.

SYNOPTIC INTERPRETATION

The ability of the APQ-39 radar to detect 77 percent of the total cloud encountered during operations suggests the possibility of radar identification of synoptic patterns. The recognition of air masses, frontal zones, and cyclones is feasible whenever the characteristics are reflected in the associated cloud structure. Boucher, in investigation of 1.25 cm radar, [10] has found that 85 percent of wintertime occurrences of precyclonic, cold front or trough, or post-cyclonic synoptic patterns could be readily classified. Data collected with the APQ-39 radar exhibits a similar classification. Table 7 illustrates the echo characteristics which are typical of well-defined winter air masses and frontal zones. Examples of these are shown in Figure 10. Figure 10a illustrates the limited, well-defined echo in Continental Polar air. Figure 10b shows the mixed stratified and cellular condition typical of Maritime Polar air. The continuous stratified echo experienced in Maritime Tropical air is illustrated in Figure 10c.

Figure 10d shows the well-defined base and indefinite top characteristic associated with echo in the proximity of a cold front. The echo in Figure 10e reflects the rapid approach of a weak warm front with the overrunning pictured at half-hour intervals as uniform stratified echo lowering and gradually

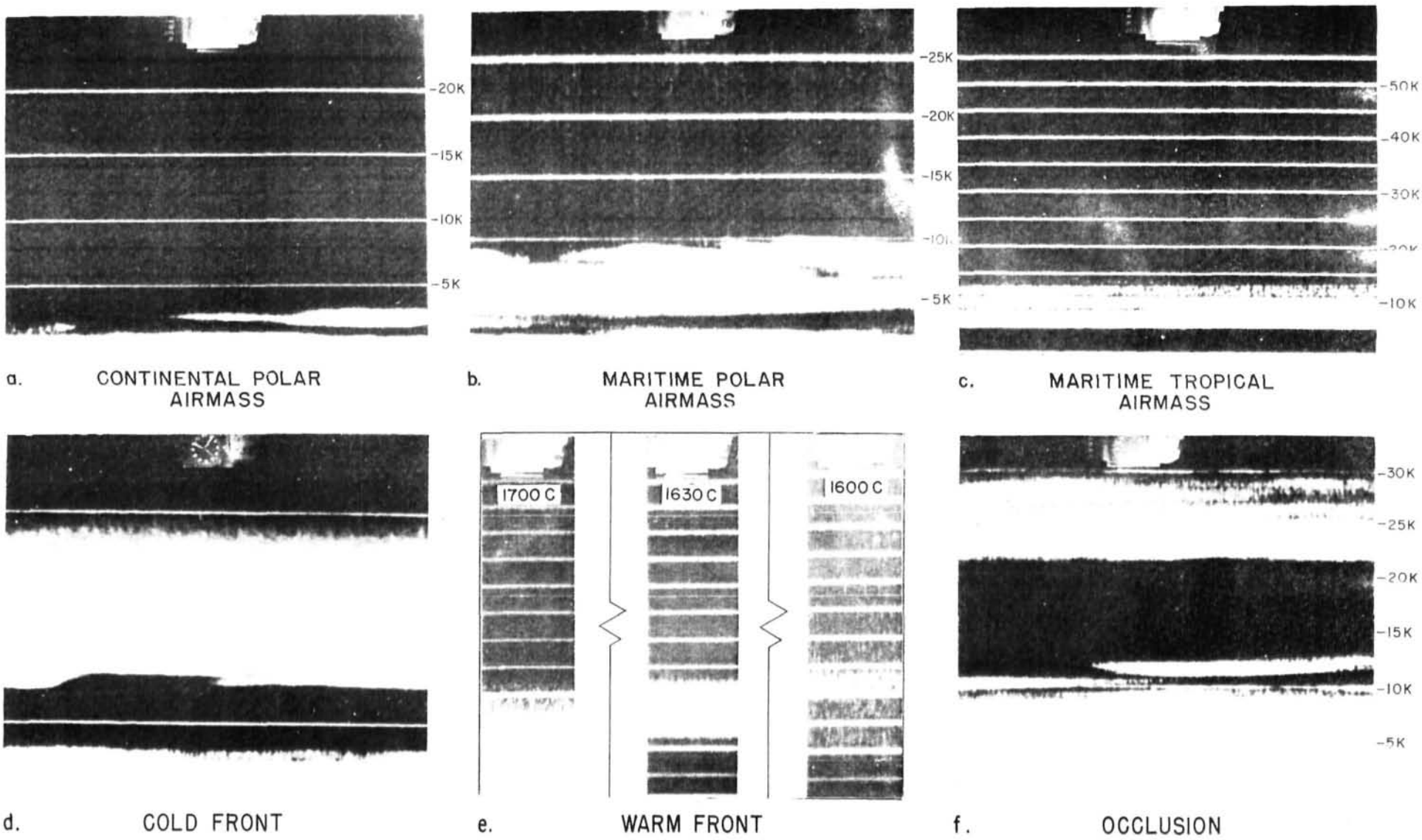

FIG. 10 AIRMASSES AND FRONTS AND ASSOCIATED RADAR ECHOES

TABLE 7

CHARACTERISTICS OF RADAR ECHOES

ASSOCIATED WITH VARIOUS WINTER AIR MASSES AND FRONTAL ZONES

Air Mass	Frontal zones	Character of echo	Average depth of echo	Continuity of echo	Echo Boundary-	Remarks
Maritime tropical		Stratified	10,000'	Continuous	Indef-inite	Echo exhibits uniform bands
Maritime polar		Stratified -cellular	10,000'	Continuous	Indef-inite	Generally stratified with embedded cells
Continen-tal polar		Cellular	10,000'	Broken	Sharp	Echo appears almost coherent clusters of cell
	Warm	Stratified	20,000'	Continuous	Indef-inite top, sharp base	Initially broken multilayers, thick-ening and lowering with top streamers continually merging with main layer. Base remains ragged until precip. begins
	Cold	Cellular	20,000'	Broken	Indef-inite top, sharp base	Non-uniform echo heavy but short in duration
	Occlu-sion	Stratified -cellular	30,000'	Broken	Indef-inite	Great vertical variation of stratified echo

thickening. The last illustration, Figure 10f shows the heavy cirrus overrunning, altocumulus, and lower dense stratus which were associated with an occlusion.

An example of the types in composite form is illustrated in the analysis of the intense cyclone of February 26, 27, and 28, 1958. Continuous radar operation throughout the period afforded a complete cross-section of the transgressing air-masses. Representative portions of the APQ-39 radar data are shown in the perspective drawing of the cyclone in Figures 11, 12 and 13. Available TPS-10 and CPS-9 radar data are included in the illustrations to complete the radar perspective.

The low pressure cell progressed from Missouri across Illinois and into Michigan. The first composite shows the occlusion approaching the radar site with the pre-frontal shower activity vividly illustrated by the radar presentation. The second composite illustrates the transition zone near the cyclone center. The two radar recordings show the thin stratified condition changing to a post-cyclonic condition as the low center moved northeastward. The third composite (Figure 13) presents the cross section in the northwest flow.

Summary

The APQ-39 radar has proved to be an excellent indicator of cloud and vertical moisture distributions. It has demonstrated the ability to detect 87 percent of low clouds, 75 percent of middle clouds, and 54 percent of high clouds experienced in the

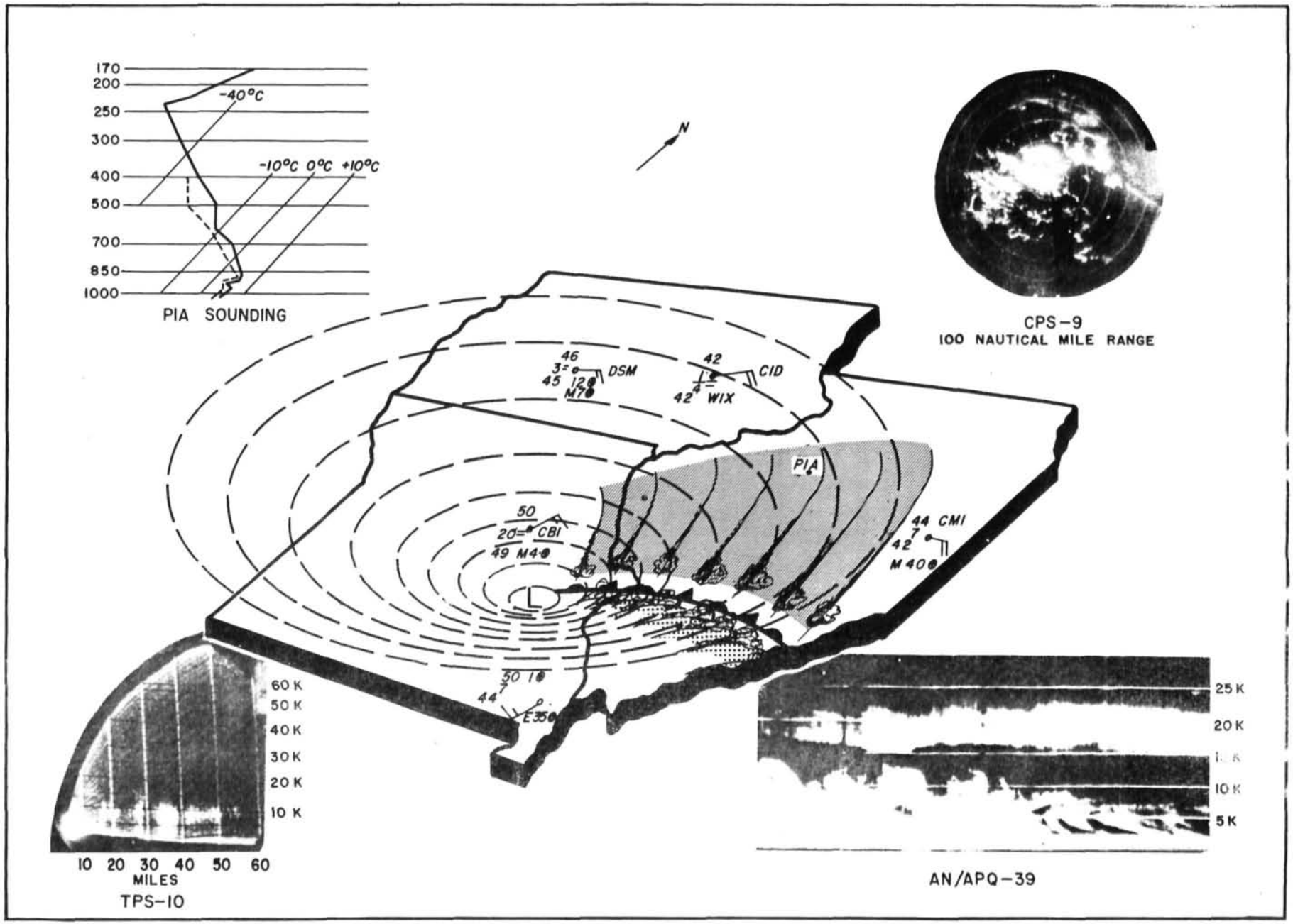

FIG. II RADAR AND SYNOPTIC COMPOSITE
0600 CST 27 FEBRUARY 1958

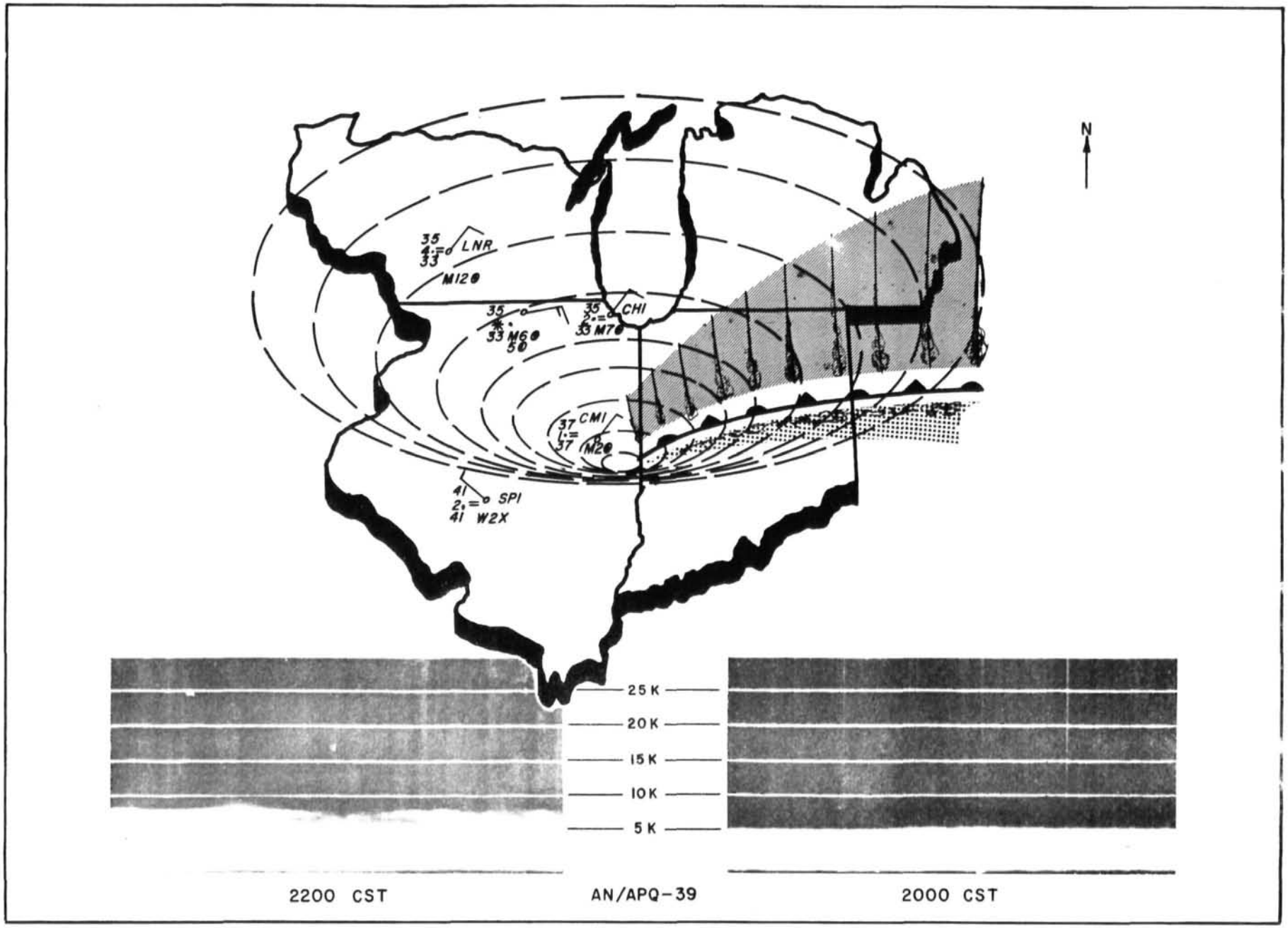

FIG. 12 RADAR AND SYNOPTIC COMPOSITE
2100 CST 27 FEBRUARY 1958

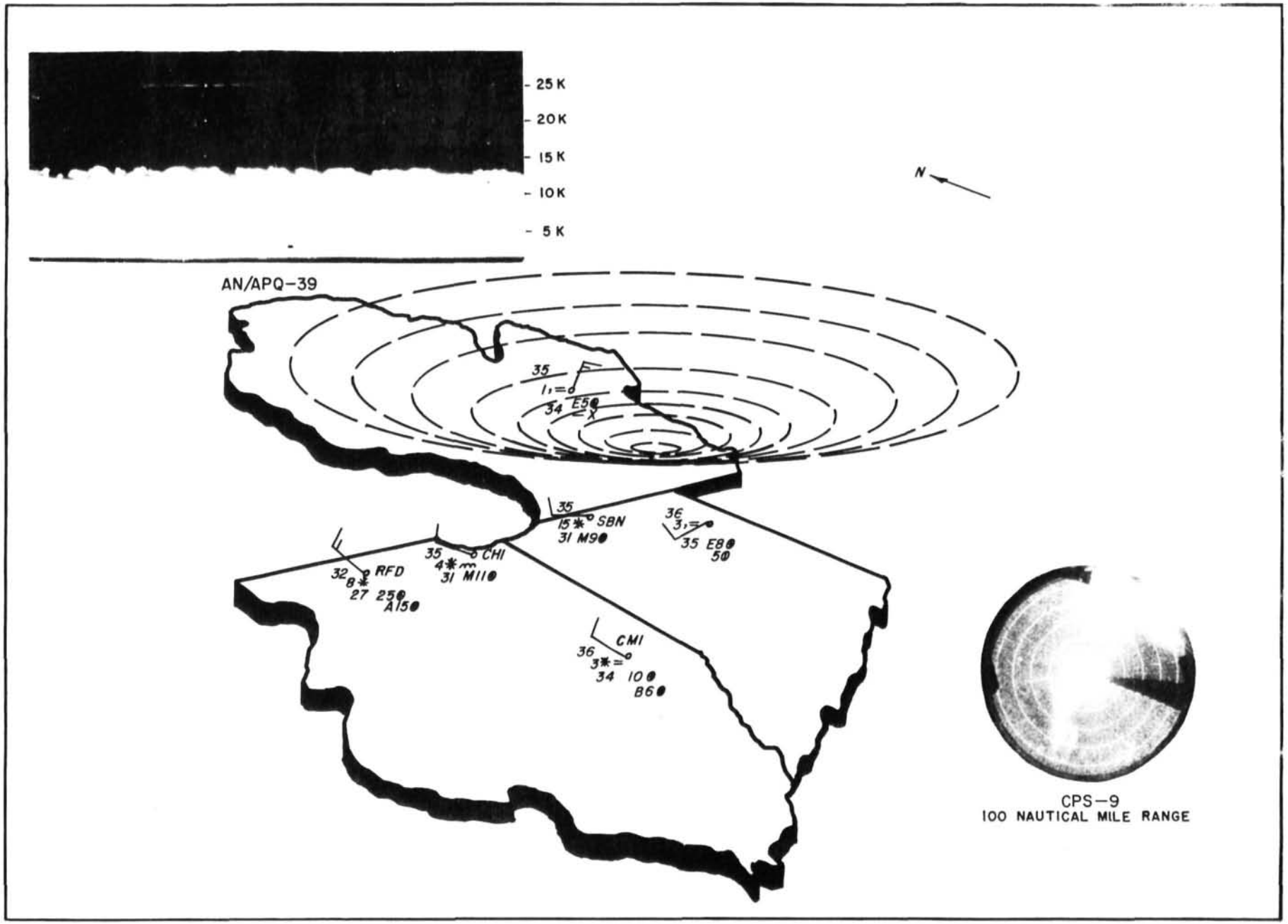

FIG. 13 RADAR AND SYNOPTIC COMPOSITE

1200 CST 28 FEBRUARY 1958

Midwest during the winter months. The detectability is superior to that of 1.25 cm wavelength radar as investigated by Plank in which the percentages were found to be 55, 52, and 28 respectively. Echo characteristics are generally analogous to cloud genera and therefore permit good reliability in data interpretation. Limited data indicate the radar is superior to balloon observations for the measurement of cloud bases. The APQ-39 radar is extremely sensitive to the detection of surface precipitation. The effect of rain attenuation on cloud return becomes noticeable when the rate exceeds approximately five mm/hr.

The radar exhibits great potential as an aid in subjective air mass and frontal analysis. The echo presentation can be incorporated with 3 cm radar RHI and PPI presentations to provide useful 3-dimensional radar perspectives of cloud and precipitation.

The author believes that further investigation will establish the cloud detection radar as an integral part in research and operational radar monitoring of meteorological phenomena.

REFERENCES

1. Plank, V. G., Atlas, Do, and Paulsen, W. H., "The Nature and Detectibility of Clouds and Precipitation as Determined by 1.25 cm Radar," J. Meteorology. 12, 1958, 358-378.

2. Leasure, R. B., and Thompson, G. A., CWO, Flight Test Results of Cloud Base and Top Indicator. AN/APQ-39(XA-1), WADC Technical Report 53-398, Wright Air Development Center, Dayton, Ohio, September, 1953, 64pp.

3. Changnon, S. A., Jr., and Huff, F. A., Cloud Distribution and Correlation with Precipitation in Illinois, Report of Investigation 33, Illinois State Water Survey, Urbana, Illinois, 1957, 83pp.

4. Robbiani, R. L., and Swingle, D. M., Effect of Collimation on a Two-Antenna Radar System. Engineering Report 1177, Signal Corps Engineering Laboratories, 15 May 1956, 12pp.

5. Austin, P. M., Note on Comparison of Ranges of Radio Set SCR-615-B and Radar Set AN/TPS-10A for Storm Detection, Technical Report 5, Weather Radar Research, Cambridge, Massachusetts Institute of Technology, 1947, 12pp.

6. Willett, Hurd C, American Air Mass Properties, Massachusetts Institute of Technology and Woods Hole Oceanographic Institution, Cambridge, Massachusetts, 1933, ll6pp.

7. Ryde, J. W., The Attenuation and Radar Echoes Produced at Centimeter Wavelengths by Various Meteorological Phenomena; Meteorological Factors in Radio Wave Propagation, The Physical Society, London, 1946.

8. Haddock, F. J., Scattering and Attenuation of Microwave Radiation Through Rain, Naval Research Laboratory, Washington, D. C., (unpublished manuscript), 1948.

9. Bartnoff, S., and Atlas, Do, "Microwave Determination of Particle-size Distribution," J. Meteorology, 8, 1951, 130-131.

10. Boucher, R. J., Synoptic - Physical Implications of 1.25 cm Vertical Beam Radar Echoes, Meteorological Radar Studies No. 5, Blue Hill Meteorological Observatory, Harvard University, 1957, 24pp+24pp.